Molecular Crystals and Liquid Crystals
Publication details, including instructions for authors and subscription information:
http://www.tandfonline.com/loi/gmcl20

Influence of Photoconductivity on the Photorefractive Effect of Ferroelectric Liquid Crystal Mixtures

A. Katsuragi [a], E. Inoue [a] & T. Sasaki [a]
[a] Department of Chemistry, Faculty of Science, Tokyo University of Science, Tokyo, Japan

Version of record first published: 07 Oct 2011

To cite this article: A. Katsuragi, E. Inoue & T. Sasaki (2011): Influence of Photoconductivity on the Photorefractive Effect of Ferroelectric Liquid Crystal Mixtures, Molecular Crystals and Liquid Crystals, 548:1, 107-119

To link to this article: http://dx.doi.org/10.1080/15421406.2011.590333

Mol. Cryst. Liq. Cryst., Vol. 548: pp. 107–119, 2011

ISSN: 1542-1406 print/1563-5287 online
DOI: 10.1080/15421406.2011.590333

Taylor & Francis
Taylor & Francis Group

Influence of Photoconductivity on the Photorefractive Effect of Ferroelectric Liquid Crystal Mixtures

A. KATSURAGI, E. INOUE, AND T. SASAKI*

Department of Chemistry, Faculty of Science, Tokyo University of Science, Tokyo, Japan

The influence of photoconductivity on the photorefractive effect of ferroelectric liquid crystals (FLCs) was investigated. Mixtures of phenylpyrimidine derivatives, a chiral dopant, and a viscosity reducer were used as host FLC materials and two types of photoconductive compounds and an electron acceptor compound were added. The photorefractive effect was evaluated using two-beam coupling experiments. It was found that the magnitude of the gain coefficient was affected by the difference between the mobility of the photoconductive compound and that of the electron acceptor.

Keywords Charge separation; ferroelectric liquid crystals; mobility; photoconductivity; photorefractive effect

1. Introduction

The photorefractive effect is a phenomenon in which the refractive index of a material is periodically modulated on the basis of photogenerated charge redistribution. When two laser beams interfere in a photorefractive material, a refractive index grating is formed. The phase of a refractive index grating resulting from the photorefractive effect does not coincide with that of the interference fringe. In the case that the phase of the refractive index grating is shifted from the interference fringe, two interfering beams result in an asymmetric energy exchange, in that the transmitted intensity of one beam increases, while that of the other beam decreases [1,2]. The refractive index grating formed through the photorefractive effect is a dynamic hologram. The photorefractive effect is expected to realize various optical devices, including real-time holographic display [1,3–7]. The photorefractive effect of ferroelectric liquid crystals (FLCs) has been reported [8–13]. FLCs exhibit a chiral smectic C phase (SmC*) that possesses a helical structure [14]. When the FLC is sandwiched between glass plates to provide a film a few micrometers thick, the helical structure is uncoiled and a surface-stabilized state (SS-state) is formed in which spontaneous polarization appears. An FLC doped with a photoconductive compound exhibits a photorefractive effect. The interference of two laser beams in an FLC doped with a photoconductive compound induces the generation of positive and negative charges at the

*Address correspondence to T. Sasaki, Department of Chemistry, Faculty of Science, Tokyo University of Science, 1-3 Kagurazaka, Shinjuku-ku, Tokyo 162-8601, Japan. E-mail: sasaki@rs.kagu.tus.ac.jp

light positions of the interference fringe, and the resultant charges drift or diffuse within the material. A charge-separated state is formed in the material due to the difference in the mobilities of the positive and negative charges. The bright and dark positions of the interference fringe are charged with opposite polarities, and thus an internal electric field (space charge field) is generated in the area between the bright and the dark positions. The resultant internal electric field changes the direction of the spontaneous polarization at the corresponding area. Thus, a refractive index grating based on the periodical change in the directors of the FLC molecules is formed (Fig. 1). It has been previously reported that the photorefractive effect of FLCs has a fast response time of 18 ms with application of a low voltage of 0.1–0.2 V/μm [9–14]. However, it is not yet well understood how the structure and the physical properties of FLCs affect the photorefractive effect.

In this study, FLC mixtures with different photoconductive properties were prepared and the influence of the photoconductivity on the photorefractive effect was investigated.

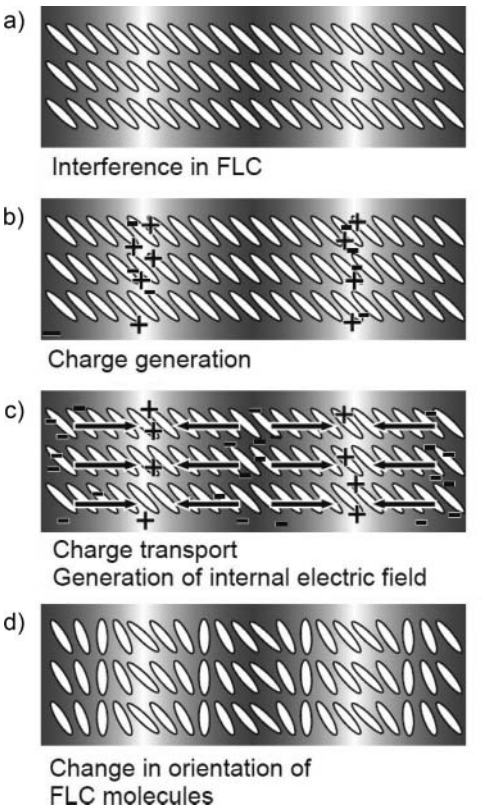

Figure 1. Schematic illustration of the mechanism for the photorefractive effect in FLCs: (a) two laser beams interfere in the surface-stabilized state of the FLC/photoconductive compound mixture, (b) charge generation occurs in the bright areas of the interference fringes, (c) the photogenerated charges are separated by diffusion in the presence of an external field and an internal electric field is generated between the bright and dark positions due to the difference in the mobilities of the positive and negative charges, and (d) the orientation of the spontaneous polarization vector (i.e., orientation of mesogens) is altered by the internal electric field.

2. Experimental

Samples

The structures of the compounds used in this study are shown in Fig. 2. Three different liquid crystals (LCs) that possess the phenylpyrimidine structure were mixed to obtain a base LC that exhibits the SmC phase over a wide temperature range. In order to impart ferroelectricity to the base LC, the chiral dopant 8BP-Iso was mixed with the base LC. Cyclo10 was added to the mixture as a viscosity reducer. Hereafter, the mixture of phenylpyrimidine LC, 8BP-Iso (2 wt%), and Cyclo10 (2 wt%) is referred to as base FLC. The base FLC was mixed with two types of photoconductive compounds and the electron acceptor trinitrofluorenone (TNF) was also added (Table 1). The prepared samples were injected into a sandwich glass cell equipped with 1-cm^2 indium tin oxide (ITO) electrodes and a polyimide alignment layer (LX-1400, Hitachi Chemicals Co.). The gap of the cell was 2 or 10 μm, as determined by a glass spacer. In order to obtain a uniformly aligned LC phase, the prepared samples were heated to the isotropic phase temperature and then cooled down to room temperature at a rate of 0.5°C/min.

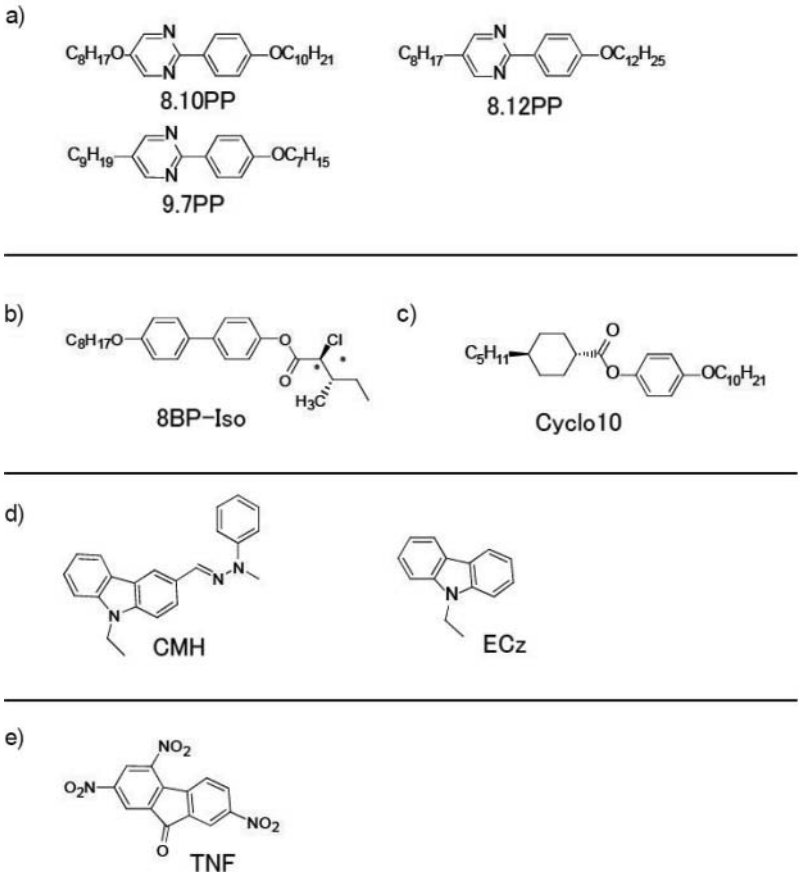

Figure 2. Structures of the compounds used in this study: (a) liquid crystals with phenylpyrimidine (PP) moiety (8.10PP, 8.12PP, and 9.7PP), (b) chiral dopant (8BP-Iso), (c) viscosity reducer (Cyclo10), (d) photoconductive compounds (CMH and ECz), and (e) electron acceptor (TNF).

Table 1. Composition of the photorefractive FLCs examined in this study

Base LC[a] (wt%)	8BP-Iso (wt%)	Cyclo10 (wt%)	CMH (wt%)	ECz (wt%)	TNF (wt%)
94	2	2	2	—	0.1
94	2	2	2	—	0.2
94	2	2	2	—	0.3
94	2	2	2	—	0.4
94	2	2	—	2	0.1
94	2	2	—	2	0.2
94	2	2	—	2	0.3
94	2	2	—	2	0.4

[a]Mixture of 8.10PP, 8.12PP, and 9.7PP (1:1:1) (PP, phenylpyrimidine).

Measurements

The phase-transition temperatures of the samples were measured using differential scanning calorimetry (DSC; DSC822 Mettler), and a polarizing optical microscope (POM; BX-50, Olympus, with FP-80 and FP-82 hot stage, Mettler) was used to observe the textures. Absorption spectra were measured using UV-Visible (UV-Vis) spectrometer (U-2800, Hitachi). The magnitude of the spontaneous polarization was measured using the triangular-waveform voltage method ($10V_{p\text{-}p}$, 100 Hz). The switching time $T_{10\text{–}90}$ was measured using the POM, an oscilloscope, and a function generator with application of a $10V_{p\text{-}p}$ square-waveform voltage. The photoconductivity was measured using an Ar^+ laser and an ultra-high resistance meter (R8340A, Advantest). The photorefractivity was measured by a two-beam coupling (2BC) experiment, which was performed using a p-polarized Ar^+ laser (165LGS-S, Laser Graphics, 488 nm, continuous wave, 2.5 mW, 1-mm diameter); the experimental setup is shown in Fig. 3. The outer and inner incident beam angles to the glass plane were 40° and 60°, respectively. The interval of the interference fringe (Λ) was calculated to be 1.70 μm according to the following equation:

$$\Lambda = \frac{\lambda}{2n \sin(\theta/2)}, \tag{1}$$

where λ is the wavelength, n is the refractive index of the sample ($n = 1.65$), and θ is the angle between the incident laser beams. The photorefractive effects were measured with direct current (DC) voltage applied to the sample to promote the charge separation efficiency.

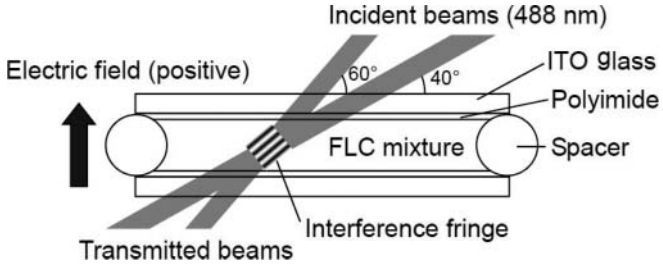

Figure 3. Schematic illustration of the beam incidence condition in the two-beam coupling experiment.

3. Results and Discussion

3.1 Influence of the TNF Concentration on Photoconductivity

The influence of the photoconductive compounds and the TNF concentration on the photorefractive effect of the FLCs was investigated. The phase-transition temperatures of the FLC mixtures are shown in Fig. 4 as a function of the TNF concentration. The SmC^* phase was observed over a wide temperature range, including the ambient temperature in both the

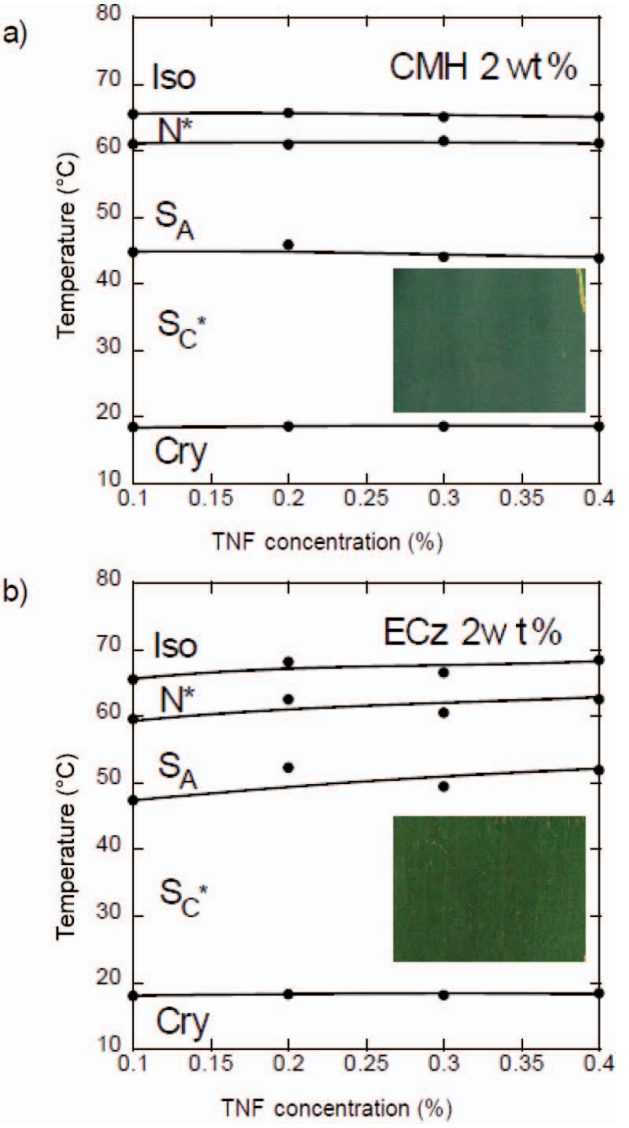

Figure 4. Phase diagrams of the FLC mixtures doped with TNF. The FLC mixture is a mixture of the base LC (94 wt%), 8BP-Iso (2 wt%), Cyclo10 (2 wt%), and the photoconductive compound (a) CMH (2 wt%) or (b) ECz (2 wt%). Inset photographs show the textures observed under the POM.

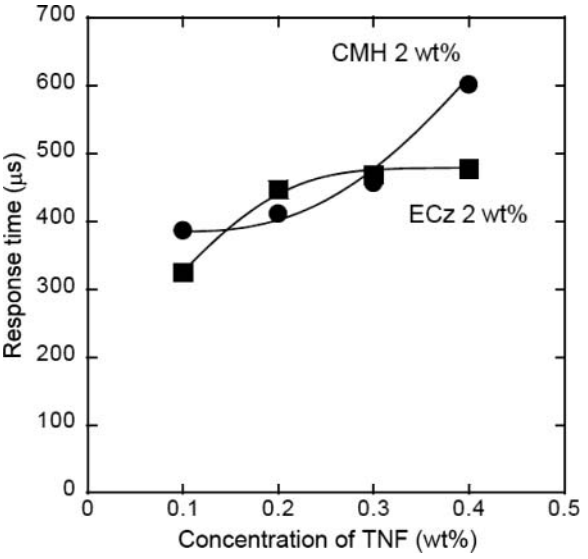

Figure 5. Dependence of the response time in the electro-optical switching of the FLC mixtures on the TNF concentration, which was varied from 0.1 wt% to 0.4 wt%. The FLC mixture was a mixture of the base LC (94 wt%), 8BP-Iso (2 wt%), Cyclo10 (2 wt%), and the photoconductive compound CMH (2 wt%) or ECz (2 wt%).

CMH (2 wt%) and the ECz (2 wt%) samples. Both of these samples retained the SS-state with few defects. The dependence of the electro-optical switching response time of the samples on the TNF concentration is shown in Fig. 5. The samples showed response times of 300–600 μs. The electro-optical response became slower as the concentration of TNF was increased. The absorption spectra of the samples with various TNF concentrations are shown in Fig. 6. As the concentration of TNF was increased, the absorption at 488 nm (wavelength of the Ar^+ laser) was increased due to the formation of a charge-transfer complex between the carbazole moiety of the photoconductive compound and TNF. The mixtures of FLC, photoconductive compound, and TNF exhibited spontaneous polarizations smaller than 1 nC/cm^2. The dependence of the applied electric field on the photocurrent and dark current of the sample with 2 wt% CMH/0.4 wt% TNF and that of the sample with 2 wt% ECz/0.4 wt% TNF are shown in Fig. 7. There was almost no difference between the photocurrents of the CMH and ECz samples. On the other hand, the dark current of the CMH sample was lower than that of the ECz sample. It was considered that the carriers responsible for the dark current are not only the photoconductive dopants but also other ionic species that could not be removed in the purification process.

3.2 Influence of the TNF Concentration on the Photorefractive Effect

The photorefractivity of the samples was measured by a 2BC experiment. Figure 8 shows a typical example of the asymmetric energy exchange observed in the mixture of base FLC, CMH, and TNF under an applied DC electric field of 0.1 V/μm. Interference of the divided beams by the sample resulted in increased transmittance of one beam and decreased transmittance of the other. The change in the transmitted intensities of the two beams was completely symmetric, as can be seen in Fig. 8. This result suggests that the phase of

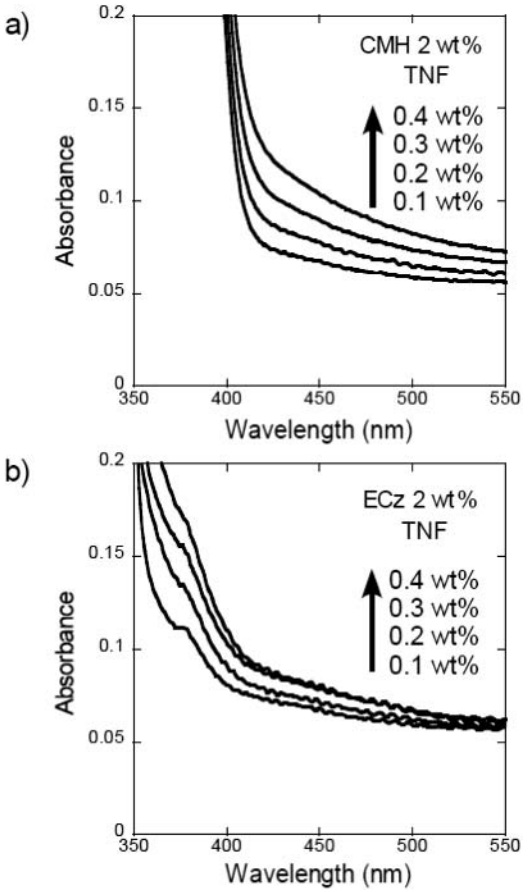

Figure 6. Absorption spectra of the photoconductive compound and TNF in the FLC mixture measured in a 10-μm gap LC cell. The concentration of TNF was 0.1 wt% to 0.4 wt%. The FLC mixture was a mixture of the base LC (94 wt%), 8BP-Iso (2 wt%), Cyclo10 (2 wt%), and the photoconductive compound (a) CMH (2 wt%) or (b) ECz (2 wt%).

the refractive index grating is shifted compared with that of the interference fringe [1–3]. The diffraction condition is characterized by the nondimensional parameter Q, which was calculated according to the following equation:

$$Q = \frac{2\pi\lambda D}{n\Lambda^2}, \tag{2}$$

where D is the interaction path length.

When $Q > 1$, the diffraction is in the Bragg regime, and when $Q < 1$, the diffraction is in the Raman–Nath regime. A Q value greater than 10 is usually required to guarantee that diffraction occurs entirely in the Bragg regime. The Q value for our experiment was calculated to lie in the range of 6–8. Therefore, the diffraction observed in this study occurred predominantly, but not entirely, in the Bragg regime but had a small Raman–Nath component. The magnitude of the photorefractive effect was estimated by the gain coefficient,

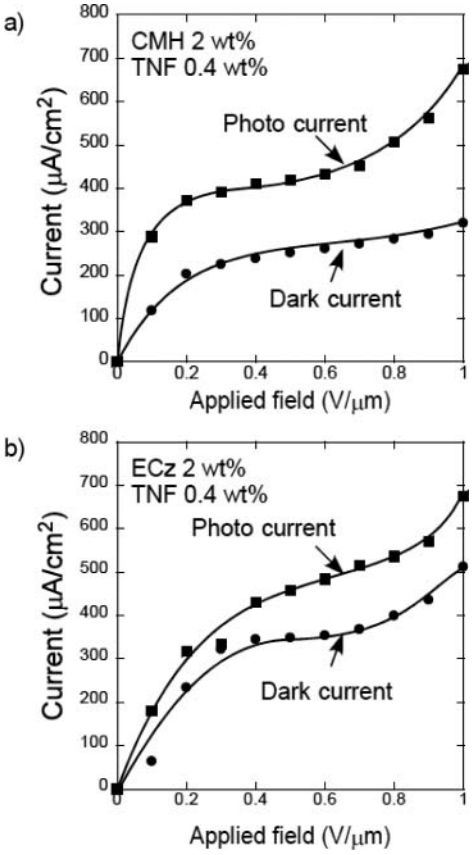

Figure 7. Dependence of the photocurrent and dark current of the mixtures of photoconductive compounds, TNF and FLC, measured in a 10-μm gap LC cell as a function of the external electric field. The concentration of the photoconductive compound (a) CMH or (b) ECz was 2 wt%, and that of TNF was 0.4 wt%. An electric field of 0.1 V/μm was applied. A 488-nm Ar^+ laser was used as the irradiation source. The power of the laser was 10 mW/cm^2.

which was calculated as follows:

$$\Gamma = \frac{1}{D} \ln \left(\frac{gm}{1 + m - g} \right), \tag{3}$$

where m is the ratio of the beam intensities (pump/signal) in front of the sample, and g is the ratio of the signal beam intensities (with pump/without pump) behind the sample. The dependence of the gain coefficient on the applied electric field for the CMH/TNF and ECz/TNF samples is shown in Fig. 9. As the concentration of TNF in the CMH sample was increased, the magnitude of the gain coefficient increased. It was considered that the strength of the internal electric field increased with the TNF concentration. In contrast, the gain coefficient of the ECz sample was independent of the TNF concentration; the strength of the internal electric field in the ECz sample was not dependent on the TNF concentration. As shown in Fig. 6, the difference in the change in absorbance at 488 nm upon addition of TNF was not significant when comparing the CMH and ECz samples.

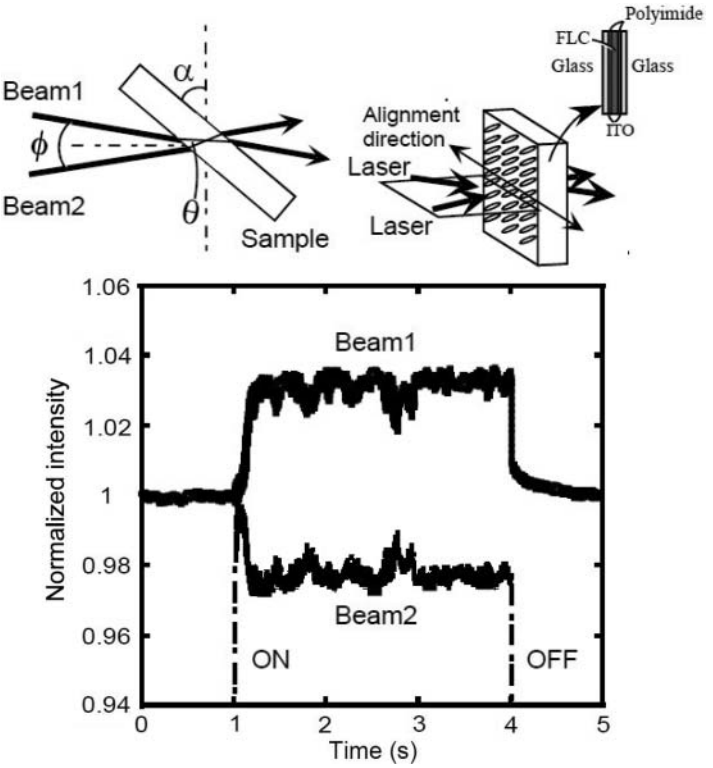

Figure 8. Typical example of asymmetric energy exchange observed in the mixture of base FLC, CMH, and TNF. An electric field of 0.1 V/μm was applied. The sample angle α was 50°, and the intersection angle φ was 20°. The shutter was opened at $t = 1$ s and closed at $t = 4$ s.

Therefore, the results shown in Fig. 9 cannot be explained based on this difference. The results indicate that the mechanism for the formation of the internal electric field in the FLC material is based on ionic conduction. The molecular lengths of CMH, ECz, and TNF were estimated to be 15.4, 9.3, and 9.9 Å, respectively (Fig. 10). The difference in the molecular length between CMH and TNF is larger than that between ECz and TNF. Therefore, it is considered that the difference in the mobilities of CMH and TNF in the FLC medium is larger than that between ECz and TNF. The difference in the mobilities of the positive and negative charges results in charge separation. Low-mobility species remain in the bright areas of the interference fringe and high-mobility species move to the dark area. Thus, the large difference in the mobilities of the positive and negative charges results in a large internal electric field. The large difference in the mobility between CMH cation and TNF anion resulted in larger diffraction efficiency than that in the ECz/TNF samples. The mechanism for the photorefractive effect of FLCs is based on the change in the direction of the spontaneous polarization; therefore, a large internal electric field leads to a large photorefractive effect.

The difference between the photocurrent and the dark current is slightly larger in the CMH sample than in the ECz sample as shown in Fig. 6 even though the mobility of the ECz cation is, as discussed previously, found to be larger than that of CMH. While the difference in the mobility of the charge carriers contributes to the photorefractive gain, the difference in

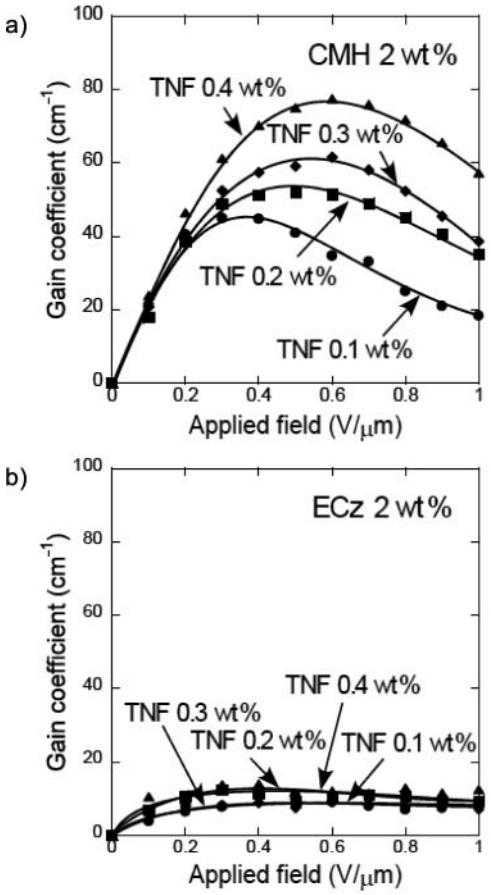

Figure 9. Dependence of the gain coefficient as a function of the external electric field for (a) CMH and (b) ECz photoconductive compounds. The concentration of TNF was varied from 0.1 wt% to 0.4 wt%.

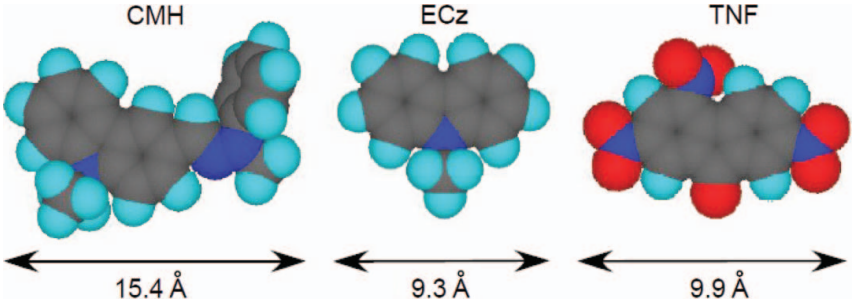

Figure 10. The molecular lengths of the photoconductive compounds estimated by MOPAC calculation.

the number of the carriers contributes to the magnitude of the photocurrent. The results in Fig. 6 indicate that the number of the carriers produced under photoirradiation is larger in the CMH sample. The difference in the absorption at 488 nm between the CMH sample and the ECz sample is small and cannot explain the difference in the gain coefficients shown in Fig. 9; however, the difference in the absorption explains the difference in the number of the carriers produced under photoirradiation. Thus, it can be considered that the small difference in the photoconductivity between the CMH sample and the ECz sample is explained by the small difference in the absorption at 488 nm, and the large difference in the photorefractive property between the CMH sample and the ECz sample cannot be explained by the absorption however be explained by the difference in the mobility of the photogenerated ionic species.

In this study, the formation time of the refractive index grating was also investigated. The intensity of the amplified transmitted laser beam in the 2BC experiment was fitted by

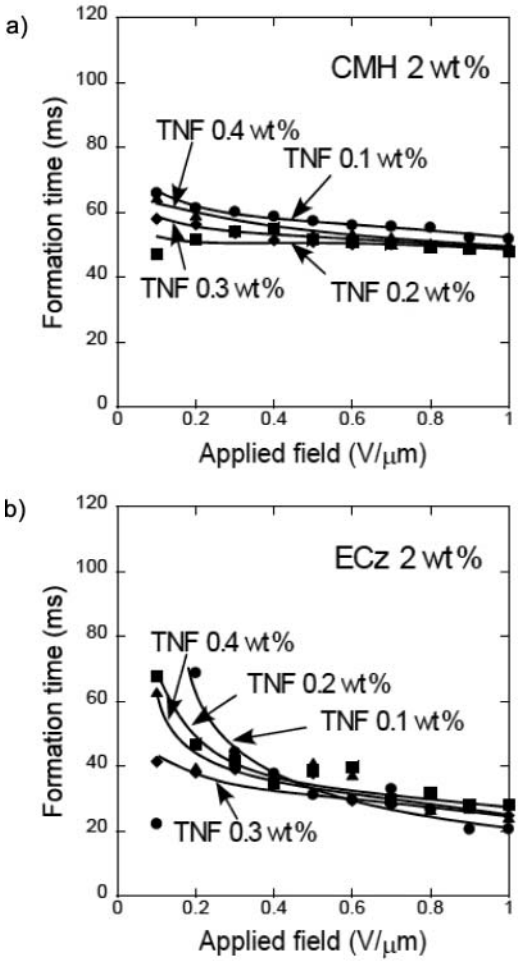

Figure 11. Refractive index grating formation time as a function of the external electric field for (a) CMH and (b) ECz photoconductive compounds. The concentration of TNF was varied from 0.1 wt% to 0.4 wt%.

the following equation:

$$r(t) = r\left[1 - \exp\left\{\frac{t}{\tau}\right\}\right]^2. \tag{4}$$

The dependence of the formation time on the applied electric field in the CMH/TNF and ECz/TNF samples is shown in Fig. 11. The response time of the CMH/TNF sample was almost independent of the applied electric field. A response time of 50 ms was obtained with application of an external electric field at 0.1 V/μm. On the other hand, as the applied electric field was increased, the formation of the index grating in the ECz/TNF sample became faster; a formation time of 30 ms under 0.1 V/μm was obtained for the ECz/TNF sample. The formation time of the ECz/TNF sample was faster than that of the CMH/TNF sample because the mobility of ECz is larger than that of CMH. However, although the concentration of TNF in the CMH/TNF and ECz/TNF samples was increased, the formation time did not vary. It was considered that the formation time was not affected by the concentration of TNF because the formation time of the charge distribution is dependent on the mobility of the charge but not on the amount of the charge. The results shown in Figs 8 and 9 clearly indicate that the mechanism of the photorefractive effect in FLCs mixed with photoconductive compounds is based on ionic conduction.

4. Conclusion

The influence of the photoconductive compounds and the concentration of the electron acceptor TNF on the photorefractive effect in FLCs was investigated. The gain coefficient of the CMH/TNF sample was larger than that of the ECz/TNF sample, and it was found that the 2BC gain coefficient was dependent on the difference between the mobility of the photoconductive compound and that of TNF.

Acknowledgments

This work was supported by the Japan Science and Technology Agency (JST)' S-Innovation. The authors would like to thank the Canon Foundation for financial support.

References

[1] Yeh, P. (1993). *Introduction to Photorefractive Nonlinear Optics*, John Wiley & Sons: New York.
[2] Moerner, W. E., & Silence, S. M. (1994). *Chem. Rev.*, *94*, 127.
[3] Kleina, M. B., Bachera, G. D., Jepsen, A. G., Wright, D., & Moerner, W. E. (1999). *Opt. Commun.*, *162*, 79.
[4] Goonesekera, A., Wright, D., & Moerner, W. E. (2000). *Appl. Phys. Lett.*, *76*, 3358.
[5] Joo, W. J., Kim, N. J., Chun, H., Moon, I. K., & Kim, N. (2001). *Poly. J.*, *42*, 9863.
[6] Joo, W. J., & Kim, N. J. (2004). *Poly. J.*, *36*, 674.
[7] Chen, F. S. (1967). *J. Appl. Phys.*, *38*, 3418.
[8] Fukuda, A., & Takezoe, H. (1990). *Structure and Properties of Ferroelectric Liquid Crystals*, Corona Press: Tokyo.
[9] Wiederrecht, G. P., Yoon, B. A., & Wasielewski, M. R. (2000). *Adv. Mater.*, *12*, 1533.
[10] Sasaki, T., Kino, Y., Shibata, M., Mizusaki, N., Katsuragi, A., Ishikawa, Y., & Yoshimi, Y. (2001). *Appl. Phys. Lett.*, *78*, 4112.
[11] Sasaki, T., Katsuragi, A., Mochizuki, O., & Nakazawa, Y. (2003). *J. Phys. Chem. B*, *107*, 7659.

[12] Talarico, M., Termine, R., Prus, P., Barberio, G., Pucci, D., Ghedini, M., & Golemme, A. (2005). *Mol. Cryst. Liq. Cryst.*, *429*, 65.
[13] Talarico, M., & Golemme, A. (2006). *Nat. Mater.*, *5*, 185.
[14] Moriya, N., & Sasaki, T. (2008). *J. Phys. Chem. C*, *111*, 17646.